Azonine, a "Nearly" Forgotten Aromatic Molecule

K. R. F. Somers,[†] E. S. Kryachko,[‡,§] and A. Ceulemans*[,†]

Department of Chemistry, University of Leuven, Celestijnenlaan 200 F, B-3001 Leuven, Belgium, and Bogoliubov Institute for Theoretical Physics, Kiev, 03143 Ukraine

Received: October 9, 2003; In Final Form: February 25, 2004

The theoretical study of azonine (C_8NH_9) and its *N*-substituted derivatives presents a new view on the azonine chemistry. Azonine is characterized as a molecule with very specific aromatic properties: interaction with surrounding H_2O molecules and alkali ions and substitution of the N−H hydrogen distorts the planarity of the ring. This distortion is such that the aromaticity remains. *N*-Methylazonine is characterized as nonplanar and the global minimum structures of the alkali salts have the metal residing on top of the distorted ring (cation−π interaction). These findings explain the experimentally known ^{1}H NMR spectra, UV−vis spectra, and thermal stability studies. The study also includes the reaction paths from azonine to *cis*- and *trans*-8,9-dihydroindole, and suggests that the trans isomer could be formed by proper kinetic control. The vibrational spectrum of azonines, analyzed with the potential energy distribution approach, is presented for the first time.

1. Introduction

1*H*-Azonine (Az) is a nine-membered heterocyclic molecule that is considered to be aromatic[1−6] being a planar, monocyclic system fulfilling the Hückel $4n + 2$ rule[7] ($n = 2$ for azonine). It is an interesting system as the planarity breaking steric strain of the ring atoms almost overcomes the planarity enforcing aromaticity, such that azonine is believed to exist in both the planar and the distorted conformation when it is solvated in acetone at room temperature.[8]

No further experimental research has been performed on this molecule, and its *N*-substituted derivatives, since the pioneering ^{1}H NMR, UV−vis, and thermal stability studies by Anastassiou (see ref 8 and references therein). The first computational study of azonine,[9] using the MNDO approach, was carried out in 1986, and the more recent theoretical studies only consider it as a reference system.[10−12]

The current work presents a thorough theoretical study of azonine and its water complexes to explain the previously mentioned experimental results of Anastassiou. It includes the determination of the geometries, the NICS values, and the singlet electronic excitation spectra. The first complete assignment of azonines vibrational spectrum is included, and the effects of water binding are discussed.

Both the methylated *N*-derivative and the alkali azonide salts are also considered, because their experimental behavior is quite different from that of azonine. The former, *N*-methylazonine (1Me-Az), is less thermally stable than azonine, but still has aromatic properties. The latter are more thermally stable than azonine and are believed to be more planar and therefore more aromatic. These variations of azonine are compared with the parent structure and the experimental findings are reevaluated with the aid of the theoretical analysis.

* Corresponding author. E-mail: arnout.ceulemans@chem.kuleuven.ac.be.
† University of Leuven.
‡ Bogoliubov Institute for Theoretical Physics.
§ Present address: Department of Chemistry, University of Liège, Sart-Tilman, B-4000 Liège, Belgium. E-mail: eugene.kryachko@ulg.ac.be.

2. Computational Methodology

All geometry optimizations were performed with the hybrid density functional B3LYP potential in conjunction with a 6-31+G(d) (≡ A) basis set, as implemented in GAUSSIAN98.[13] This level is adequate for the geometry optimization of aromatic compounds as stated in ref 14 and references therein. The azonine geometry was further refined for comparison with a 6-311++G(2d,2p) (≡ B) basis set. The harmonic vibrational frequencies and zero-point vibrational energies (ZPVE) were calculated at the B3LYP/A level to construct potential energy surfaces (PESs), and to provide a complete assignment of the azonine vibrational modes. This assignment is based on the concept of potential energy distributions (PEDs)[15] evaluated via the GAR2PED program.[16] All mentioned energies have been corrected for the ZPVE unless stated otherwise.

The isotropic magnetic susceptibility was determined for the global minima of azonine and *N*-methylazonine, using the gauge-independent atomic orbital method,[17−19] with both the A and B basis set, as implemented in GAUSSIAN98. These calculations are performed on points located at the unweighted geometry center of the ring (NICS(0)) and 1 Å above this point for planar geometries[20] (NICS(1)). The harmonic oscillator measure of aromaticity (HOMA) values[21] were also calculated to include a structural measure of aromaticity.

The singlet valence excitation energies were determined with the complete active space self-consisting-field (CASSCF) method[22] combined with a second-order perturbation formalism[23] (CASPT2) as implemented[24] in MOLCAS4.0. This CASPT2 calculation was performed on the wave function obtained after averaging over the first 9 roots of the CASSCF calculation. An atomic natural orbital[25] (ANO-S) type basis set contracted to (C,N 3s2p1d/H 2s1p) was used, supplemented with a 3p3d set of Rydberg functions. These Rydberg functions are constructed from eight primitives of each angular momentum type, and are built following the standard procedure.[26] The active space of azonine (C_{2v} symmetry) contains 4 valence orbitals of A_2 symmetry and 5 valence orbitals of B_2 symmetry. Inclusion

10.1021/jp037046+ CCC: $27.50
Published on Web 04/14/2004

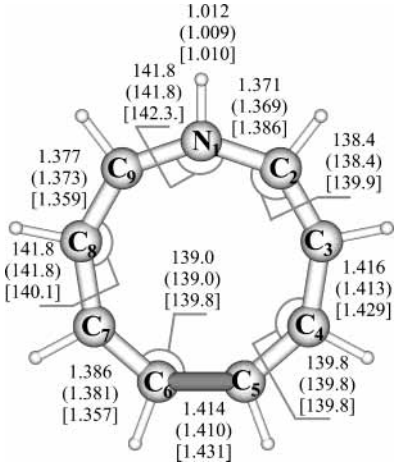

Figure 1. Ground-state geometry of azonin. Bond lengths are indicated in Å and bond angles in deg. The displayed values are from top to bottom: B3LYP/A, B3LYP/B, and MNDO.[9]

of the Rydberg function is necessary to correctly describe valence excitations. Singlet excitations were also determined by using an extended active space that contains in addition one A_1 and one B_1 type orbital. The small active space was also applied in the analogous calculations of the planar azonine−H_2O complex, the planar Li-azonide, and the distorted *N*-methylazonine.

3. Results and Discussion

3.1. Azonine. The optimized structure of azonine is displayed in Figure 1. The B3LYP/A, B3LYP/B, and MNDO[9] geometrical parameters are added. The atom numbering displayed in Figure 1 is used throughout the entire discussion.

Azonine is a planar molecule of C_{2v} symmetry with a dipole moment of 3.0 D (vs 2.54 D as predicted by MNDO[9]) that lies on the C_2 axis and points from the center of the ring toward the nitrogen atom. The HOMO−LUMO energy gap of azonine is equal to 4.56 eV, which is 1.78 times smaller than the value determined with MNDO,[9] but corresponds well with the B3LYP/6-311G(2d,p) value[27] of 4.57 eV.

The harmonic vibrational modes of azonine are gathered in Tables 1−3, and are presented, for the first time, with the appropriate assignments based on PED patterns. Three specific modes are important for the further discussion: the ν_{NH} stretch centered at 3596 cm^{-1}, and the symmetric and asymmetric stretches, $\nu_{C2(9)H}$, of 3182 and 3183 cm^{-1}, respectively. Deuterium substitution of one of the C−H groups downshifts the ν_{CH} frequency to 2345 cm^{-1}.

The deviation of the dihedral angle $\angle C_2N_1C_5C_6$ from its planar value, also referred to as $\angle C_2N_1C_5C_6$, is used to indicate the degree of ring distortion. The deviation value is 0.0° for the planar gas-phase azonine. The N−$C_{2(9)}$ distance of 1.371 Å is shorter than the average single bond N−C distance of 1.47 Å and longer than the average N═C double bond distance[28] of 1.30 Å. The C_n−C_{n+1} distances vary between 1.377 and 1.416 Å and are therefore very similar to the average benzene value[28] of 1.400 Å. These distances combined with the planarity of the system clearly suggest that azonine is aromatic, although the C_n−C_{n+1} bond length alternation around the average benzene value shows slightly polyenic properties.

While a detailed investigation of aromaticity requires close scrutiny of current densities under external magnetic field[29] we limit our analysis to the NICS[20] and the HOMA[21] values which provide a practical numerical measure. Azonines aromaticity is confirmed by the NICS(0) values of −13.262 and −13.215 ppm, for respectively the A and B basis set (NICS(1) = −11.891 ppm with A and −12.010 ppm with B), which are in accordance with the values of Salcedo et al.,[27] who determined NICS(0) to be equal to −12.836 ppm using B3LYP/6-311G(2d,p). These values fit well between the benzene and pyrrole benchmark values[20] of respectively −9.7 and −15.1 ppm (B3LYP/6-31+G-(d), and clearly indicate that azonine is aromatic. Similar results are obtained for the HOMA of azonine which equals 0.900 at the A level and 0.909 at the B level. These values also fit well between the benzene and pyrrole benchmark values of respectively 1.000 and 0.876.

The experimental excitation maxima and singlet valence excitations of azonine are presented in Table 4. The applied solvents are seen to have a large effect on the spectrum. The correspondence between the experimental *n*-hexane (C_6H_{14}) maxima and the theoretical values is reasonably good for both the standard calculation and the calculation with the extended basis set. The theoretically determined lowest energy excitation of 3.58 eV is slightly lower than the experimental value of 3.70 eV, but still within the accepted error margin for this type of calculation. The next theoretical peak is at 4.20 eV; it is characterized by low oscillator strength and not observable in the experimental spectrum. The intense high-energy experimental maximum of 4.92 eV is assigned to the theoretical excitations around ∼5.5 eV, because these values have a very large oscillator strength. The 5.10 eV excitation has a weak oscillator strength and is therefore not attributed to the intense experimental peak of 4.92 eV. It is interesting though because it is the only excitation of the $\pi \rightarrow \sigma^*_{NH}$ type instead of $\pi \rightarrow \pi^*$.

The other experimental spectra have to be considered with some care because of the profound effect of the solvent on the spectrum. Replacing C_6H_{14} by diethyl ether (Et_2O), which has weak hydrogen bonding capacities, already complicates the spectrum dramatically. More hydrogen bonding media like THF, ether, methanol, and water shift the low-energy excitation band[4] from 3.70 to ∼4.00 eV. It is clear that the theoretical azonine results alone are incapable of explaining the spectroscopic data. The calculations are therefore extended to azonine−water complexes to simulate the effects of more polar media. The azonide salts are also included (Li and Na) to explain the similarities between the K-azonide and the azonine (Et_2O) spectrum. We will return to this part of the azonine discussion in the azonine−H_2O section.

Azonine, and the other thermally labile heteronins, rearrange exclusively to the cis-fused bicycle[4] ($C_{2(9)}$ and $C_{7(4)}$ connect). The corresponding PES is shown in Figure 2 and the structural parameters are given in Table 5. The global minimum structure is *cis*-8,9-dihydroindole (**Cis**) and it lies 10.5 kcal/mol below azonine and 9.5 kcal/mol below *trans*-8,9-dihydroindole (**Trans**). The rearrangement from azonine to **Cis** proceeds through a transition state (**TS_1**) with an activation barrier of 30.8 kcal/mol. It is a straightforward, Woodward−Hoffmann allowed,[5] one-step reaction that is unlikely to occur easily at ambient temperature. This result agrees well with the original experimental findings of Anastassiou,[1] who did not observe changes after prolonged heating at 34 °C. The rearrangement from azonine to **Trans** proceeds via a two-step process. The first transition state (**TS_2**) has an activation energy of 16.1 kcal/mol and leads to a local minimum (**Int**) that resides 17.8 kcal/mol above the global minimum. **Int** is only slightly distorted from planarity and is characterized by the swapping of the C_2−H hydrogen atom to the inside of the ring. This displacement,

TABLE 1: Harmonic Vibrational Modes of Azonine and Their Assignment Using PED Analysis[a]

C_{2v}	no.	freq, cm^{-1}	IR, km/mol	assignment, PED, %
A_2	1	42	0	$\tau_2(39)$, $\tau_1(19)$
B_2	2	98	2	$\tau_1(41)$, $\gamma N_1H(11)$, $\gamma C_8H(10)$, $\gamma C_3H(10)$
A_1	3	269	~0	$\beta_2(89)$
B_1	4	274	0	$\beta_1(88)$
B_2	5	379	~0	$\tau_4(67)$
A_2	6	418	0	$\tau_3(69)$
B_2	7	577	47	$\tau_5(48)$, $\tau_6(17)$, $\gamma N_1H(10)$
A_2	8	648	0	$\tau_6(54)$, $\tau_5(16)$
B_2	9	649	157	$\tau_5(26)$, $\gamma C_2H(16)$, $\gamma C_9H(16)$, $\gamma C_4H(10)$, $\gamma C_7H(10)$,
A_1	10	651	~0	$\beta_4(68)$, $\beta_3(23)$
B_1	11	670	~0	$\beta_3(70)$, $\beta_4(23)$
A_1	12	691	2	$\nu C_3C_4(14)$, $\nu C_7C_8(14)$, $\nu N_1C_2(13)$, $\nu N_1C_9(13)$, $\nu C_5C_6(11)$
B_2	13	711	~0	$\gamma N_1H(52)$
A_2	14	752	0	$\gamma C_9H(23)$, $\gamma C_2H(23)$, $\gamma C_8H(16)$, $\gamma C_3H(16)$
B_2	15	817	~0	$\gamma C_2H(20)$, $\gamma C_9H(20)$, $\gamma N_1H(23)$
B_1	16	871	8	$\nu C_3C_4(24)$, $\nu C_7C_8(24)$, $\nu C_8C_9(12)$, $\nu C_2C_3(12)$
A_2	17	871	0	$\gamma C_7H(22)$, $\gamma C_4H(22)$, $\gamma C_9H(19)$, $\gamma C_2H(19)$
A_1	18	880	13	$\nu C_5C_6(24)$, $\nu N_1C_2(18)$, $\nu N_1C_9(18)$, $\nu C_6C_7(11)$, $\nu C_4C_5(11)$
B_1	19	924	3	$\beta_6(86)$, $\beta_5(12)$
B_2	20	942	~0	$\gamma C_3H(20)$, $\gamma C_8H(20)$, $\gamma C_2H(15)$, $\gamma C_9H(15)$
A_2	21	952	0	$\gamma C_8H(25)$, $\gamma C_3H(25)$, $\tau_3(10)$
A_1	22	953	3	$\beta_5(81)$, $\beta_6(10)$
B_2	23	991	~0	$\gamma C_7H(23)$, $\gamma C_4H(23)$, $\gamma C_8H(10)$, $\gamma C_3H(10)$
A_2	24	1016	0	$\gamma C_5H(25)$, $\gamma C_6H(25)$, $\gamma C_4H(14)$, $\gamma C_7H(14)$, $\tau_6(12)$
A_1	25	1200	4	$\nu C_5C_6(21)$, $\nu C_7C_8(15)$, $\nu C_3C_4(15)$, $\nu N_1C_9(10)$, $\nu N_1C_2(10)$
B_1	26	1233	0	$\nu N_1C_2(13)$, $\nu N_1C_9(13)$, $\nu C_4C_5(12)$, $\nu C_6C_7(12)$
B_1	27	1431	~0	$\beta C_7H(21)$, $\beta C_4H(21)$
A_1	28	1436	5	$\beta C_5H(16)$, $\beta C_6H(16)$, $\beta C_8H(10)$, $\beta C_3H(10)$, $\nu C_8C_9(10)$, $\nu C_2C_3(10)$
A_1	29	1448	8	$\beta C_6H(12)$, $\beta C_5H(12)$
B_1	30	1483	~0	$\beta C_6H(14)$, $\beta C_5H(14)$, $\beta C_4H(13)$, $\beta C_7H(13)$, $\beta C_8H(13)$, $\beta C_3H(13)$
A_1	31	1495	6	$\beta C_3H(14)$, $\beta C_8H(14)$, $\nu C_5C_6(13)$, $\nu C_4C_5(11)$, $\nu C_6C_7(11)$
A_1	32	1529	3	$\beta C_7H(23)$, $\beta C_4H(23)$, $\beta C_9H(12)$, $\beta C_2H(12)$
B_1	33	1530	~0	$\beta C_8H(19)$, $\beta C_3H(19)$, $\nu N_1C_9(11)$, $\nu N_1C_2(11)$
B_1	34	1534	~0	$\beta C_2H(38)$, $\beta C_9H(38)$
A_1	35	1586	3	$\beta C_2H(16)$, $\beta C_9H(16)$, $\nu C_5C_6(12)$
B_1	36	1604	18	$\beta N_1H(39)$, $\nu N_1C_2(17)$, $\nu N_1C_9(17)$
B_1	37	1654	0	$\nu C_6C_7(21)$, $\nu C_4C_5(21)$
A_1	38	1684	16	$\nu C_8C_9(16)$, $\nu C_2C_3(16)$, $\nu C_5C_5(12)$
B_1	39	1697	1	$\beta N_1H(29)$, $\nu C_2C_3(17)$, $\nu C_8C_9(17)$, $\nu C_3C_4(10)$, $\nu C_7C_8(10)$
B_1	40	3112	~0	$\nu C_5H(32)$, $\nu C_6H(32)$, $\nu C_4H(15)$, $\nu C_7H(15)$
A_1	41	3120	~0	$\nu C_7H(28)$, $\nu C_4H(28)$, $\nu C_3H(13)$, $\nu C_8H(13)$
B_1	42	3129	~0	$\nu C_8H(27)$, $\nu C_3H(27)$, $\nu C_5H(13)$, $\nu C_6H(13)$
A_1	43	3139	16	$\nu C_8H(27)$, $\nu C_3H(27)$, $\nu C_5H(17)$, $\nu C_6H(17)$
B_1	44	3150	69	$\nu C_7H(26)$, $\nu C_4H(26)$, $\nu C_3H(16)$, $\nu C_8H(16)$
A_1	45	3158	58	$\nu C_5H(24)$, $\nu C_6H(24)$, $\nu C_4H(18)$, $\nu C_7H(18)$
B_1	46	3182	28	$\nu C_2H(45)$, $\nu C_9H(45)$
A_1	47	3183	18	$\nu C_9H(44)$, $\nu C_2H(44)$
A_1	48	3596	53	$\nu N_1H(100)$

[a] PEDs less than 10% are not included. Symmetry coordinates for the bending β and torsion τ modes are defined in Tables 2 and 3.

which is impossible for smaller ring systems, makes the reaction to **Trans** also Woodward−Hoffmann allowed, because it therefrom proceeds exactly like the cis reaction. The reaction reaches **Trans** via a transition state, **TS_3**, with an activation barrier of 25.6 kcal/mol. The opposite reaction, from **Trans** to **Int**, requires an activation energy of 33.9 kcal/mol. The described reaction scheme suggests that **Trans** could be formed by proper kinetic control. The calculated enthalpy differences between **Cis** and the other local minima are 10.9 kcal/mol for azonine, 18.0 kcal/mol for **Int**, and 9.4 kcal/mol for **Trans**. The corresponding entropy differences are 3.6, 1.0, and −1.2 cal/(mol·K), respectively. Heating the sample results therefore only in small Gibbs free energy changes between the molecules and does not influence the relative thermodynamics much.

3.2. Azonine−H_2O. Placing water molecules at different positions above the azonine plane and at the N−H hydrogen bond position results in two stable complexes, shown in Figure 3. Both complexes are expected because azonine has a hydrogen bond donation group N−H (Az-w[1]) and an aromatic ring, the π-electron cloud of which acts as a π-hydrogen bond acceptor (Az-w[2]). The former, σ-type complex has a binding energy of 5.8 kcal/mol, versus 3.5 kcal/mol for the π-type complex.

Formation of the N−H···O hydrogen bond retains the planarity of Az-w[1]. The N−H bond length increases slightly by 0.006 Å and results in a 92-cm^{-1} bathochromic shift of the ν_{NH} stretching vibration, the IR intensity of which is enhanced by a factor of 11.

Formation of the π-type complex Az-w[2] through the $O-H_1\cdots C_4$ and $O-H_2\cdots C_6$ bonds, with bond lengths of 2.874 and 2.886 Å, respectively, modestly affects the planarity of azonine, shown by the $\angle C_2N_1C_5C_6$ value of 12.5°. The O−H bonds of the water molecule are slightly increased (0.002 Å) because of the hydrogen bond formation. Both O−H groups are bound to azonine, thereby hindering the scissor vibration of H_2O, which shifts 21 cm^{-1} to the blue. The O−H stretching vibrations, ν_1 and ν_3, are respectively shifted 22 and 39 cm^{-1} downward because of the hydrogen bonds. These small shifts suggest that the π hydrogen bond between azonine and water

TABLE 2: Symmetry Coordinates for the Bending, β, Modes of the Azonine Ring in Terms of Its Internal Ones[a]

description	coeff	atoms	description	coeff	atoms
β_1	1.00	$N_1C_2C_3$	β_2	0.98	$C_2C_3C_4$
	0.17	$C_2C_3C_4$		0.34	$C_3C_4C_5$
	−0.94	$C_3C_4C_5$		−0.87	$C_4C_5C_6$
	−0.50	$C_4C_5C_6$		−0.64	$C_5C_6C_7$
	0.77	$C_5C_6C_7$		0.64	$C_6C_7C_8$
	0.77	$C_6C_7C_8$		0.87	$C_7C_8C_9$
	−0.50	$C_7C_8C_9$		−0.34	$C_8C_9N_1$
	−0.94	$C_8C_9N_1$		−0.98	$C_9N_1C_2$
	0.17	$C_9N_1C_2$			
β_3	1.00	$N_1C_2C_3$	β_4	0.87	$C_2C_3C_4$
	−0.50	$C_2C_3C_4$		−0.87	$C_3C_4C_5$
	−0.50	$C_3C_4C_5$		0.87	$C_5C_6C_7$
	1.00	$C_4C_5C_6$		−0.87	$C_6C_7C_8$
	−0.50	$C_5C_6C_7$		0.87	$C_8C_9N_1$
	−0.50	$C_6C_7C_8$		−0.87	$C_9N_1C_2$
	1.00	$C_7C_8C_9$			
	−0.50	$C_8C_9N_1$			
	−0.50	$C_9N_1C_2$			
β_5	1.00	$N_1C_2C_3$	β_6	0.34	$C_2C_3C_4$
	−0.94	$C_2C_3C_4$		−0.64	$C_3C_4C_5$
	0.77	$C_3C_4C_5$		0.87	$C_4C_5C_6$
	−0.50	$C_4C_5C_6$		−0.98	$C_5C_6C_7$
	0.17	$C_5C_6C_7$		0.98	$C_6C_7C_8$
	0.17	$C_6C_7C_8$		−0.87	$C_7C_8C_9$
	−0.50	$C_7C_8C_9$		0.64	$C_8C_9N_1$
	0.77	$C_8C_9N_1$		−0.34	$C_9N_1C_2$
	−0.94	$C_9N_1C_2$			

[a] Numbering of the atoms is indicated in Figure 1.

TABLE 3: Symmetry Coordinates for the Torsion, τ, Modes of the Azonine Ring in Terms of Its Internal Ones[a]

description	coeff	atoms	description	coeff	atoms
τ_1	1.00	$N_1C_2C_3C_4$	τ_2	0.98	$C_2C_3C_4C_5$
	0.17	$C_2C_3C_4C_5$		0.34	$C_3C_4C_5C_6$
	−0.94	$C_3C_4C_5C_6$		−0.87	$C_4C_5C_6C_7$
	−0.50	$C_4C_5C_6C_7$		−0.64	$C_5C_6C_7C_8$
	0.77	$C_5C_6C_7C_8$		0.64	$C_6C_7C_8C_9$
	0.77	$C_6C_7C_8C_9$		0.87	$C_7C_8C_9N_1$
	−0.50	$C_7C_8C_9N_1$		−0.34	$C_8C_9N_1C_2$
	−0.94	$C_8C_9N_1C_2$		−0.98	$C_9N_1C_2C_3$
	0.17	$C_9N_1C_2C_3$			
τ_3	1.00	$N_1C_2C_3C_4$	τ_4	0.87	$C_2C_3C_4C_5$
	−0.50	$C_2C_3C_4C_5$		−0.87	$C_3C_4C_5C_6$
	−0.50	$C_3C_4C_5C_6$		0.87	$C_5C_6C_7C_8$
	1.00	$C_4C_5C_6C_7$		−0.87	$C_6C_7C_8C_9$
	−0.50	$C_5C_6C_7C_8$		0.87	$C_8C_9N_1C_2$
	−0.50	$C_6C_7C_8C_9$		−0.87	$C_9N_1C_2C_3$
	1.00	$C_7C_8C_9N_1$			
	−0.50	$C_8C_9N_1C_2$			
	−0.50	$C_9N_1C_2C_3$			
τ_5	1.00	$N_1C_2C_3C_4$	τ_6	0.34	$C_2C_3C_4C_5$
	−0.94	$C_2C_3C_4C_5$		−0.64	$C_3C_4C_5C_6$
	0.77	$C_3C_4C_5C_6$		0.87	$C_4C_5C_6C_7$
	−0.50	$C_4C_5C_6C_7$		−0.98	$C_5C_6C_7C_8$
	0.17	$C_5C_6C_7C_8$		0.98	$C_6C_7C_8C_9$
	0.17	$C_6C_7C_8C_9$		−0.87	$C_7C_8C_9N_1$
	−0.50	$C_7C_8C_9N_1$		0.64	$C_8C_9N_1C_2$
	0.77	$C_8C_9N_1C_2$		−0.34	$C_9N_1C_2C_3$
	−0.94	$C_9N_1C_2C_3$			

[a] Numbering of the atoms is indicated in Figure 1.

is rather weak. It is therefore noteworthy that the corresponding indole−water complexes form even weaker bonds, as discussed in our recent work on indole.[30] This difference can be explained by the larger dipole of azonine that is, opposite to the indole case, directed nearly collinear with the hydrogen bond and interacts therefore more strongly with the water dipole. The effect of the dipole interaction between water and indole is also visible in the position of the water hydrogen atoms that are not

TABLE 4: Experimental and Calculated Singlet Excitations of Azonine and Derivatives[a]

	E1, eV	E2, eV	E3, eV	E4, eV
experiment				
azonine[2] (C_6H_{14})	3.70[b]			4.92
azonine[3] (Et_2O)	3.60[b]	3.78[b]	4.16[b]	5.32
azonine[3] (H_2O)	∼4.00[b]			
K-Az (THF)[4]	3.66[b]	3.76[b]		>4.43
1Me-Az (C_6H_{14})[2]	4.09[b]			5.56
calculation				
azonine	3.58[c] (A_1)	4.20[c] (B_1)	5.10[c] (B_2)	5.50 (B_1)
azonine[ext]	3.47[c] (A_1)	4.18[c] (B_1)	5.20[c] (B_2)	5.54 (B_1)
				5.57 (A_1)
Az-w[1]	3.52[c]	4.10[c]	5.13[c]	5.58
Li-Az[1]	3.52[c]	4.09[c]	5.83[c]	5.87
1Me-Az	4.14[c]	(4.58−5.13)[c]		>5.26

[a] The calculation with the extended basis set is indicated by the superscript ext. C_{2v} symmetry labels are included. All energies are in eV. [b] Weak transitions. [c] Oscillator strengths below 0.1 au.

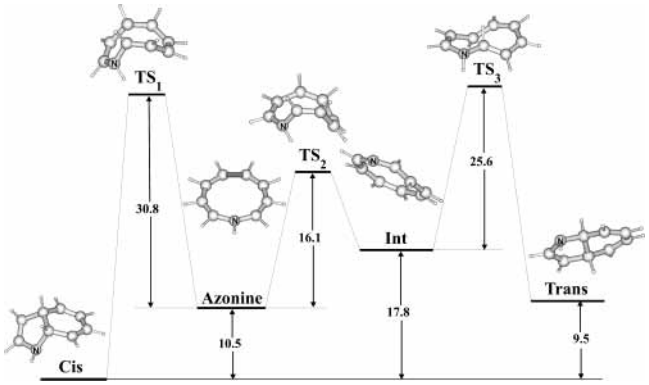

Figure 2. PES of the bicyclization of azonine. The ZPVE corrected energies are indicated in kcal/mol.

oriented along the hydrogen bond direction, but are tilted toward the dipole direction. The enlarged stability of the azonine−H_2O π-type complexes is probably due to the flexibility of the azonine ring that enhances the binding interactions. The rigid indole frame, on the contrary, does not allow this type of stabilization.

The calculated valence excitations of the planar water complex show a downshift of ∼0.08 eV for the two lowest energy excitations (see Table 4). The higher energy excitations show a similar upshift. These results are in disagreement with the experimental blue shift of 0.45 eV that is present when the solvent is changed from C_6H_{14} to water, but are in line with the indole−H_2O results that shift ∼0.07 eV compared to the uncomplexed indole.[30] Anastassiou[4] attributed the blue shift to the $N^{\delta-}-H\cdots O^{\delta+}$ interaction, which increases the effective electronegativity of the N−H function, and therefore distorts the planarity. This distortion of the planarity shifts the low-energy band to higher energies. The theoretically determined azonine−water geometries partially agree with this claim. The planarity is lost indeed, but this loss originates from the formation of the π complex. This reduced planarity affects the aromaticity as shown by the HOMA values of respectively 0.914 and 0.828 for Az-w[1] and Az-w[2]. The large blue shift is also present in the *N*-methylazonine spectrum (C_6H_{14}), a molecule that exists only in the distorted form. The shift is also present in the calculated excitation spectrum of the distorted *N*-methylazonine. Here the strong shift can indeed be attributed to the distortion from planarity. The distortion has a similar effect on the HOMA value that is 0.856 for *N*-methylazonine. The large blue shift of the lowest energy band upon solvation

TABLE 5: Geometrical Parameters of the Azonine Bicyclization[a]

	Cis	TS_1	azonine	TS_2	Int	TS_3	Trans
			bond distances				
$r(N_1-C_2)$	1.403	1.404	1.371	1.428	1.376	1.398	1.430
$r(C_2-C_3)$	1.342	1.332	1.377	1.346	1.380	1.358	1.346
$r(C_3-C_4)$	1.526	1.497	1.416	1.473	1.448	1.483	1.518
$r(C_4-C_5)$	1.514	1.404	1.386	1.351	1.406	1.463	1.506
$r(C_5-C_6)$	1.344	1.406	1.414	1.482	1.442	1.387	1.353
$r(C_6-C_7)$	1.466	1.410	1.386	1.348	1.390	1.430	1.471
$r(C_7-C_8)$	1.344	1.404	1.416	1.476	1.423	1.377	1.353
$r(C_8-C_9)$	1.508	1.402	1.377	1.344	1.361	1.414	1.500
$r(C_9-N_1)$	1.496	1.434	1.371	1.412	1.362	1.386	1.477
$r(C_9-C_4)$	1.565	2.349	4.007	3.297	2.948	2.143	1.530
			bond angles				
$\angle N_1C_2C_3$	113.4	118.5	138.4	126.8	125.0	116.5	113.9
$\angle C_2C_3C_4$	109.1	123.0	141.8	132.8	138.8	122.4	107.6
$\angle C_3C_4C_5$	113.1	122.6	139.8	133.7	145.1	140.5	127.6
$\angle C_4C_5C_6$	122.3	126.5	139.0	134.5	144.3	130.1	116.5
$\angle C_5C_6C_7$	121.3	123.7	139.0	127.0	136.4	126.5	121.2
$\angle C_6C_7C_8$	121.6	123.5	139.8	122.9	124.5	121.1	120.9
$\angle C_7C_8C_9$	121.6	123.2	141.8	122.0	113.8	114.2	115.5
$\angle C_8C_9N_1$	112.2	118.3	138.4	124.0	132.8	129.8	122.1
$\angle C_9N_1C_2$	106.4	117.0	141.8	119.8	115.0	108.1	102.9
			dihedral angles				
$\angle N_1C_2C_3C_4$	−0.4	2.9	0.0	3.5	5.8	11.7	10.0
$\angle C_2C_3C_4C_5$	107.9	93.2	0.0	31.1	−9.8	−104.8	−147.4
$\angle C_3C_4C_5C_6$	−113.8	−68.5	0.0	−5.2	7.4	104.6	158.6
$\angle C_4C_5C_6C_7$	1.1	−37.0	0.0	−69.0	8.2	4.5	−3.4
$\angle C_5C_6C_7C_8$	7.5	3.9	0.0	9.5	−7.8	−17.5	−17.4
$\angle C_6C_7C_8C_9$	1.5	38.7	0.0	61.2	−22.1	−16.3	−3.7
$\angle C_7C_8C_9N_1$	100.8	62.5	0.0	14.7	150.0	179.1	167.1
$\angle H_2C_2N_1H_1$	−38.5	58.6	0.0	93.3	33.3	53.9	68.5
$\angle H_1N_1C_9H_9$	−39.1	−133.7	0.0	−155.5	−168.5	−163.7	−152.4
$\angle H_9C_9C_4H_4$	25.8	10.5	0.0	21.3	−89.5	174.8	170.2
$\angle H_4C_4C_5H_5$	−73.0	−16.0	0.0	−0.7	3.0	36.7	96.9

[a] Bond lengths are in Å and bond angles and dihedral angles are in deg. The azonine numbering is applied for all structures.

in polar media might therefore originate from the loss of planarity induced by the solvent.

Using Et_2O as solvent gives rise to a complex spectrum. This spectrum cannot be explained by using the azonine or azonine−water calculations separately, but requires their combination. The weak maxima around ∼3.7 eV originate from both the uncomplexed and the σ-complexed spectrum. The remaining weak maximum of 4.17 eV is attributed to the distorted complex, where *N*-methylazonine also shows a weak maximum around ∼4.1 eV. The existence of distorted azonine, when solvated in acetone, was already proven by temperature-dependent ^{1}H NMR studies[8] and supports the attribution of the 4.17 eV maximum to the distorted molecule. The existence of distorted azonine, when solvated in acetone, explains why the NMR τ values of azonine[4] are between ∼3 and ∼4 ppm: the effect of the distortion on the different protons is averaged out, but the average ring current is weakened and the NMR shifts are therefore smaller than for the planar aromatic system. The azonine (Et_2O) spectrum originates therefore from three different molecules: the uncomplexed azonine, the σ complexed azonine, and the distorted azonine.

3.3. *N*-Methylazonine. The geometry optimization of the *N*-substituted azonine derivative, *N*-methylazonine (1Me-Az), results in a nonplanar molecule with a $\angle C_2N_1C_5C_6$ of 34.0°, see Figure 4. It has a dipole moment of 3.2 D, which is directed along the bond between N_1 and the carbon atom of the methyl group and points from the center of the ring toward the nitrogen atom. It actually coincides with the azonine dipole moment, but is 0.2 D larger because the methyl carbon deprives the nitrogen atom of its negative charge as shown by the Mulliken charges of respectively −0.57 au on the methyl carbon and 0.04 au on nitrogen. The methyl substitution has a noteworthy effect on the $\nu_{C2(9)H}$ stretching vibrations, shifting them to 3186 and 3209 cm^{-1} and thereby increasing their splitting to 23 cm^{-1}.

The transition state linking the 1Me-Az symmetry analogues, displayed in Figure 4, is perfectly planar, and lies only 0.6 kcal/mol above the global minimum. 1Me-Az is therefore constantly flipping through this transition state at room temperature (∼10^{12} times per second) and appears planar in ^{1}H NMR experiments. This behavior explains the measured τ values[4] of 4.15, 5.12, and 3.87−4.06 ppm that show a mild ring diamagnetism for the ring hydrogens. Comparison of the ^{1}H NMR spectra of azonine and 1Me-Az shows an upshift of ∼1 ppm for the τ values of 1Me-Az. The electron-donating mesomeric effect of the methyl substitution also changes the peak order slightly, but the peak pattern remains similar to that of azonine, which is expected as 1Me-Az is still planar on average. The strong distortion of the ring moves the hydrogens out of the plane and diminishes the ring current, which explains the increase of the τ values. The decrease of the ring current is also visible in the NICS(0) values of the nonplanar 1Me-Az. These values of −10.641 (A level) and −10.741 ppm (B level) are ∼2.5 ppm

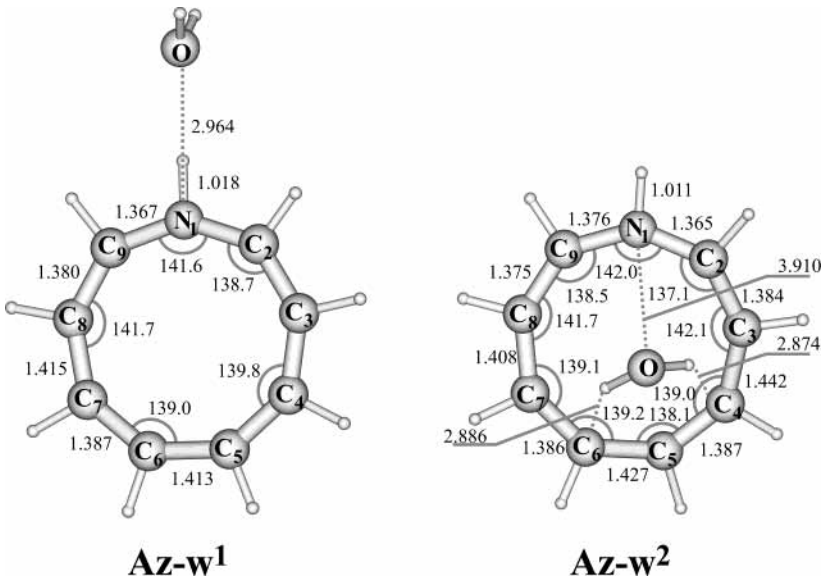

Figure 3. B3LYP/A optimized geometries of azonine−H_2O. Bond lengths are indicated in Å and bond angles in deg.

Figure 4:

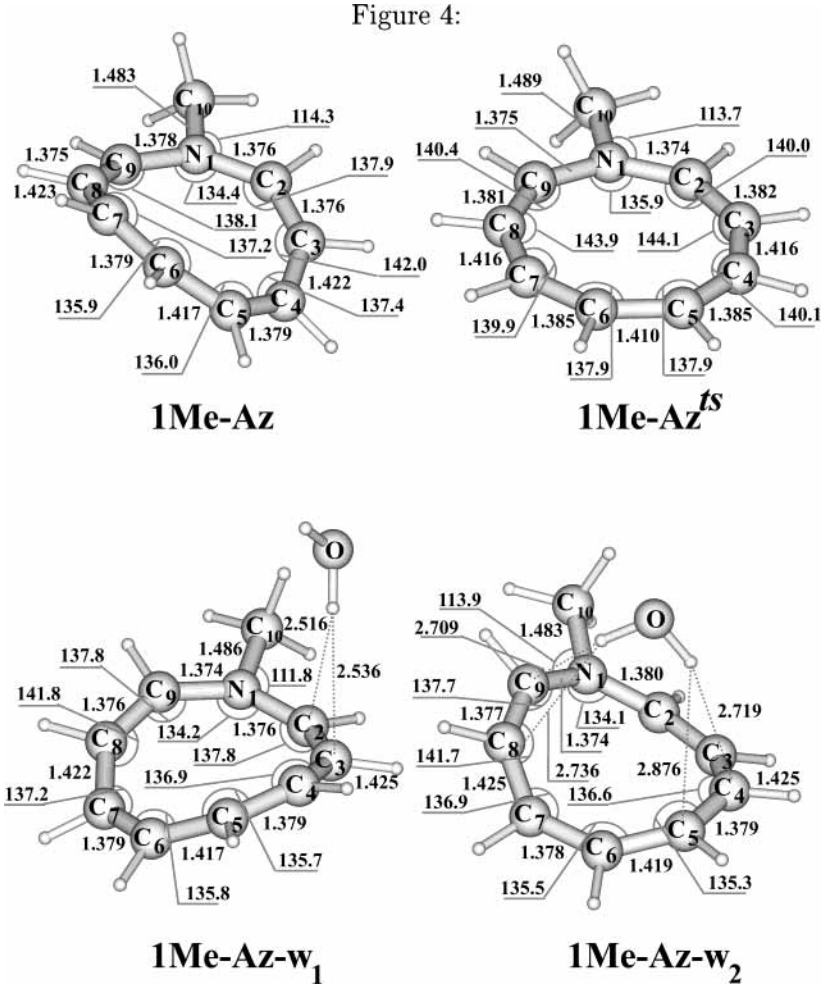

Figure 4. B3LYP/A optimized geometries of *N*-methylazonine and *N*-methylazonine−H_2O. Bond lengths are indicated in Å and bond angles in deg.

lower than the corresponding azonine values, which corresponds well with the increase of the τ values. The NICS(0) values are still close to these of benzene and pyrrole and the distorted 1Me-Az is therefore still considered aromatic. The molecular orbitals (MOs) depicted in Figure 5 support this, because they are clearly delocalized. The figure is constructed from the CASSCF wave function, after averaging over multiple states, and contains the orbitals of the applied active space. The orbitals, provided[31] by MOLCAS5.4, are visualized with MOLDEN with use of a 0.015 cutoff value. The occupation numbers are included in the picture. All depicted orbitals clearly show π character. Additional Rydberg character is present in the three orbitals with occupation numbers of 0.22 and 0.20. The position of the ring hydrogen atoms also supports the aromaticity claim because all the $\angle H_iC_iC_{i+1}H_{i+1}$ dihedral angles are ∼15°, which still allows for a complete delocalization of the π system. It is therefore interesting to note that *N*-(*N*,*N*-dimethylcarbamyl)azonine, which is characterized by $\angle H_iC_iC_{i+1}H_{i+1}$ dihedral angles of ∼90° or more, is known to be nonaromatic.[32] The singlet excitations of the nonplanar 1Me-Az are presented in Table 4 together with the experimental results. The experimentally determined energy upshift of the lowest energy absorption of 4.09 eV is also visible in the theoretical spectrum, 4.14 eV, and is of the $\pi \rightarrow \pi^*$ type. The calculations also suggest that there exist a manifold of Rydberg excitations between 4.58 and 5.13 eV. These Rydberg excitations have small oscillator strengths and are not observed in the experimental spectrum. The experimental peak at 5.56 eV corresponds to the onset of theoretical manifold of $\pi \rightarrow \pi^*$ excitations at 5.26 eV, which are characterized by large oscillator strengths. The theoretical results therefore support the statement that the distortion of the azonine ring leads to higher excitation energies of the first singlet excitation.

3.4. *N*-Methylazonine−H_2O. The *N*-methyl substitution blocks the favorable water binding site, hence binding with water is only possible through the π-electron cloud. Placing the water molecule above the *N*-methylazonine plane gives rise to two low-energy complexes: 1Me-Az-w[1] and 1Me-Az-w[2], see Figure 4. The water molecule of the 1Me-Az-w[1] complex binds to the π-electron cloud at carbon atoms C_2 and C_3, as shown by the C_2-H_w and C_3-H_w distances of 2.516 and 2.536 Å, respectively. The $\angle C_2N_1C_5C_6$ of 33.8° indicates that the planarity is somewhat restored. The water molecule of the other complex binds to azonine with two π hydrogen bonds: one leg is bonded to C_4 and C_5 (bond lengths of 2.719 and 2.876 Å, respectively) and the other to C_8 and C_9 (bond lengths of 2.736 and 2.709 Å, respectively). The $\angle C_2N_1C_5C_6$ is slightly larger than in *N*-methylazonine, 34.8° versus 34.0°.

The binding energies of the complexes are almost the same: 3.0 and 2.9 kcal/mol for respectively 1Me-Az-w[1] and 1Me-Az-w[2]. The hydrogen bonds in 1Me-Az-w[2] are, when considered separately, weaker than the 1Me-Az-w[1] hydrogen bond, as indicated by the O−H bond length increase of 0.003 and 0.002 Å for 1Me-Az-w[2], as opposed to the 0.004 Å increase in 1Me-Az-w[1]. This conclusion is supported by the ν_1 water stretch that downshifts only 30 cm^{-1} for 1Me-Az-w[2] instead of the 52 cm^{-1} for 1Me-Az-w[1]. The two weaker bonds of 1Me-Az-w[2] never-

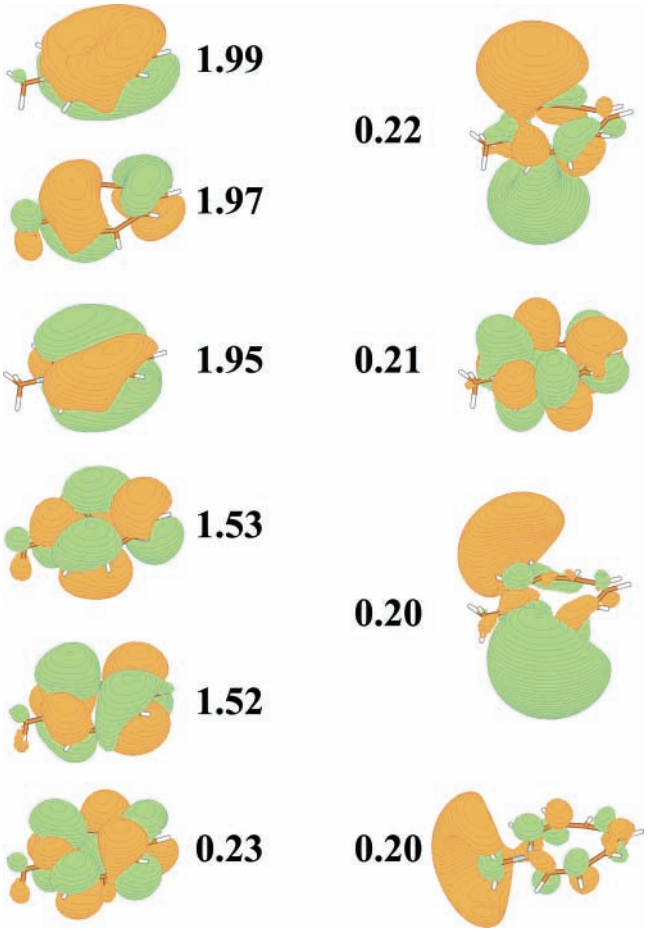

Figure 5. Molecular orbitals of the ground-state *N*-methylazonine. The numbers represent the occupation of the respective orbitals.

theless bind water as strongly as the single bond in 1Me-Az-w[1] when their total binding strength is considered.

3.5. Azonide Salts. The Li-, Na-, and K-azonides were studied experimentally,[3] including the ^{1}H NMR spectra of different azonide salts solvated in both DMSO and acetone. The thermal decomposition rates and the UV−vis spectrum of K-azonide were also recorded. Despite these previous studies no theoretical equilibrium structure has been reported so far, but it is believed that the alkali metals simply replace the hydrogen in the N-H group of azonine. The present analysis firmly demonstrates that this is not the case for Li-, Na-, and K-azonide.

The PES of Li-azonide, shown in Figure 6, contains three minima, none of which has Li at the N-H hydrogen position. In the two lowest energy minima, Li-Az[2] and Li-Az[3], Li resides above the ring. They are linked by a low-energy transition state, thus allowing Li to move almost freely above the ring. In the remaining local energy structure, Li-Az[1], Li substitutes for the N-H hydrogen, but it is shifted slightly toward the $C_{2(9)}$-H group. This structure is linked to the priorly mentioned local minima by a transition state with an activation energy of only 1.3 kcal/mol. The structural parameters of all the Li-azonide conformations are listed in Table 6.

Li-Az[1] is still a planar molecule, but the in-plane rotation of the Li atom breaks the C_{2v} symmetry of the parent azonine molecule to C_s. The displaced Li is characterized by an $\angle LiN_1C_{2(9)}$ of 87.2° and lies 23.8° off the $\angle C_9N_1C_2$ bissectrix. The specific position of Li forms an indication of its participation in two bonds: a σ-type bond with the nitrogen atom and a three-center Li···H−$C_{2(9)}$ bond. The former bond, with a bond length of 1.806 Å, is of the covalent type, as demonstrated by the Mulliken charges of 0.05 au for N and 0.26 au for Li. The latter bond is the agostic interaction[33−35] Li···H−$C_{2(9)}$ because of the specific ν_{CH} stretch changes of the involved C−H bond:[34] the azonine $C_{2(9)}$ stretches at ∼3182 cm^{-1} are shifted to 2753 and 3085 cm^{-1}. The 2753-cm^{-1} C−H stretch is mainly localized on the C−H group, which is bound to Li, and is highly IR active (332 km/mol). Deuterium substitution in this bond shifts the corresponding ν_{CH} stretch to 2345 cm^{-1} in the bare azonine and to 2022 cm^{-1} in Li-Az[1], resulting in a large red shift of 323 cm^{-1}.

The two other minimum energy structures, Li-Az[2] and Li-Az[3], have Li sitting above the plane and asymmetrically placed to the line connecting N_1 with the midpoint of the C_5−C_6 bond. Both structures are less polar in comparison with Li-Az[1]: 3.9 and 5.1 D, respectively, versus 9.0 D. Their azonine frame is

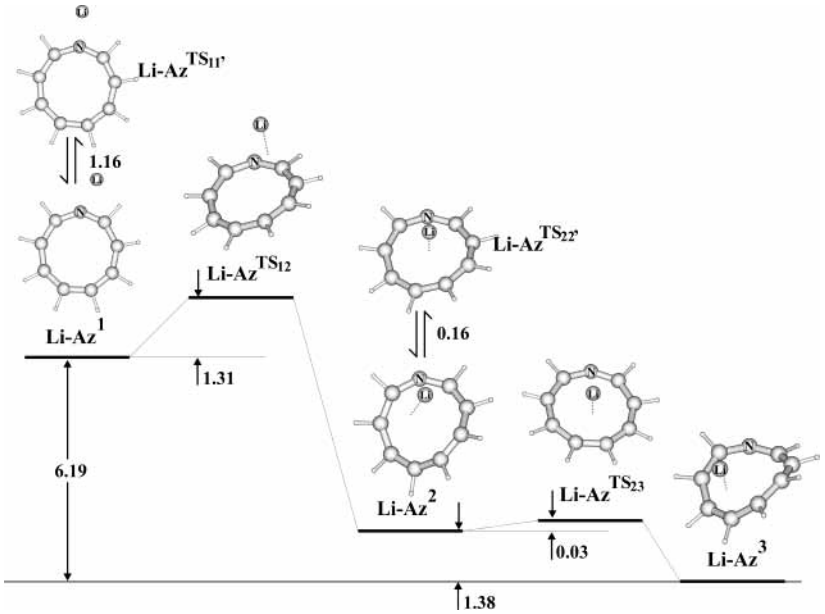

Figure 6. PES of Li−azonide The ZPVE corrected energies are indicated in kcal/mol. Li is projected on the plane that cuts symmetrically through N_1 and C_5−C_6.

TABLE 6: Geometrical Parameters, Mulliken Charges, and HOMA Values of Li-Azonide[a]

	Li-Az^1	Li-Az$^{TS_{12}}$	Li-Az^2	Li-Az$^{TS_{23}}$	Li-Az^3	Li-Az$^{TS_{11'}}$	Li-Az$^{TS_{22'}}$
				bond distances			
$r(Li-N_1)$	1.806	1.854	2.059	2.312	3.282	1.820	2.207
$r(N_1-C_2)$	1.350	1.362	1.345	1.334	1.324	1.355	1.336
$r(C_2-C_3)$	1.395	1.403	1.408	1.411	1.416	1.393	1.412
$r(C_3-C_4)$	1.408	1.408	1.425	1.413	1.426	1.411	1.416
$r(C_4-C_5)$	1.393	1.395	1.400	1.404	1.401	1.392	1.404
$r(C_5-C_6)$	1.407	1.405	1.409	1.412	1.423	1.408	1.412
$r(C_6-C_7)$	1.394	1.396	1.391	1.404	1.408	1.392	1.398
$r(C_7-C_8)$	1.409	1.407	1.410	1.413	1.408	1.411	1.412
$r(C_8-C_9)$	1.395	1.401	1.405	1.411	1.403	1.393	1.411
$r(C_9-N_1)$	1.348	1.347	1.348	1.334	1.325	1.355	1.338
				bond angles			
$\angle LiN_2C_2$	87.2	83.1	74.4	75.2	50.4	111.3	76.0
$\angle N_1C_2C_3$	143.3	140.8	135.5	138.8	137.1	141.3	137.9
$\angle C_2C_3C_4$	140.1	140.9	137.7	140.4	138.2	141.5	139.6
$\angle C_3C_4C_5$	139.4	138.8	137.3	139.6	134.6	139.8	139.0
$\angle C_4C_5C_6$	138.7	138.6	137.0	139.3	134.7	138.7	138.8
$\angle C_5C_6C_7$	139.0	138.5	135.9	139.3	136.4	138.7	138.3
$\angle C_6C_7C_8$	140.1	139.6	135.8	139.6	137.0	139.8	138.4
$\angle C_7C_8C_9$	141.7	141.1	139.6	140.4	138.1	141.5	140.4
$\angle C_8C_9N_1$	139.5	140.1	138.2	138.8	134.9	141.3	138.6
$\angle C_9N_1C_2$	138.0	137.4	137.7	143.7	137.6	137.4	142.1
				dihedral angles			
$\angle LiN_1C_2C_3$	180.0	101.7	29.2	32.0	56.4	180.0	23.3
$\angle N_1C_2C_3C_4$	0.0	7.5	13.2	0.0	−12.8	0.0	8.5
$\angle C_2C_3C_4C_5$	0.0	13.1	35.7	0.4	−38.4	0.0	17.1
$\angle C_3C_4C_5C_6$	0.0	−0.8	−5.6	1.3	3.5	0.0	−1.6
$\angle C_4C_5C_6C_7$	0.0	−11.6	−30.7	0.1	32.1	0.0	−17.1
$\angle C_5C_6C_7C_8$	0.0	−5.1	−8.0	−1.3	12.6	0.0	−4.6
$\angle C_6C_7C_8C_9$	0.0	10.5	29.3	−0.6	−31.1	0.0	17.0
$\angle C_7C_8C_9N_1$	0.0	10.1	18.0	−0.3	−24.8	0.0	7.4
				Mulliken charges			
Li	0.26	0.54	0.36	0.14	0.31	0.54	0.21
N_1	0.05	−0.09	−0.07	−0.02	−0.14	0.01	0.01
HOMA	0.956	0.946	0.907	0.903	0.865	0.947	0.903

[a] Bond lengths are in Å and bond angles and dihedral angles are in deg. The Mulliken charges are in au.

also strongly distorted: $\angle C_2N_1C_5C_6 = 34.7°$ and 43.9°, respectively. The Mulliken charges are similar: 0.36 au for Li-Az^2 and 0.31 au for Li-Az^3. These charges indicate that Li binds to the azonine part through the well-known cation$-\pi$ interaction mechanism (see refs. 36, 37, 38, 39, 40, and 41 and references therein). Li-Az^2 binds with the π cloud located at N_1, $C_{2(9)}$, and $C_{3(8)}$ with bond lengths of respectively 2.059, 2.134, and 2.169 Å. The Li of the Li-Az^3 complex binds at position $C_{3(8)}$, $C_{4(7)}$, $C_{5(6)}$, and $C_{6(5)}$, with bond lengths of respectively 2.168, 2.168, 2.157, and 2.174 Å.

The transition structures interconnecting the aforementioned local energy minima are also displayed in Figure 6, and their geometrical data are tabulated in Table 6. Li-Az^1 is linked to Li-Az^2 by the transition structure Li-Az$^{TS_{12}}$ with an activation energy of 1.3 kcal/mol and an imaginary mode of 89*i* cm^{-1}. It is characterized by the distortion of the azonine frame ($\angle C_2N_1C_5C_6 = 12.9°$) and by the out-of-plane position of Li ($\angle LiN_1C_2C_3 = 101.7°$). In the opposite direction the isomerization path has an energy barrier of 6.1 kcal/mol, implying that at room temperature Li-Az^1 is disfavored in comparison to Li-Az^2. Li-Az$^{TS_{23}}$, with an almost flat activation barrier, connects Li-Az^2 to Li-Az^3. Its structure consists of a planar azonide frame with Li residing above the plane, $\angle LiN_1C_2C_3 = 32.0°$. The imaginary mode at 20*i* cm^{-1} describes a butterfly motion of the ring. The local minima are also connected to their symmetry analogues. These transition states have activation barriers of 1.2 kcal/mol for Li-Az^1, forming a planar molecule with C_{2v} symmetry, and 0.2 kcal/mol for Li-Az^2. This last structure has Li positioned above the distorted azonide frame, $\angle LiN_1C_2C_3 = 23.3°$ and $\angle C_2N_1C_5C_6 = 17.7°$.

All three local Li-Az minima are used to determine the corresponding Na-azonide (Na-Az) and K-azonide (K-Az) geometries, see Table 7. The in-plane Na-azonide, Na-Az^1, is 12.4 kcal/mol less stable than the Na π complexes. The Na atom in Na-Az^1 is still interacting with the $C_{2(9)}$-H group, but is also shifted closer toward the $\angle C_9N_1C_2$ bissectrix. The angle $\angle NaN_1C_2$ is equal to 100.9° and Na is only 10.7° away from the bissectrix (the corresponding Li value is 23.8°.). K-Az^1 is 14.4 kcal/mol less stable than the K π complexes and shifts even more toward the bissectrix, the difference only amounts to 9.9°. The Na geometries originating from Li-Az^2 and Li-Az^3 are labeled respectively Na-Az^2 and Na-Az^3. They are almost at identical energies. The distortion of their azonine frame is smaller than that for the Li counterparts and the $\angle C_2N_1C_5C_6$ value amounts only to ~8.3°. Analogous conclusions can be drawn about K-Az^2 and K-Az^3, which have become indiscernible and are less distorted as indicated by their $\angle C_2N_1C_5C_6$ values of 2.4° and 2.6°. It is clear from these results that the azonide frame of the π-complexed salts flattens with the increase of the cation size, and that this increase of cation size moves the cations closer to the $\angle C_9N_1C_2$ bissectrix in the σ complexes. The Mulliken charges of the Li, Na, and K π complexes point to a clear increase of ionic character when the cation size increases. Only the Na and K σ complexes show ionic bond character in the σ complex. Az-Li^1 interacts covalently with the azonide frame, because its orbitals can overlap better with

TABLE 7: Geometrical Parameters, Mulliken Charges, and HOMA Values of Na- and K-Azonide and the Azonide Anion (Az^-)[a]

	Na-Az[1]	Na-Az[2]	Na-Az[3]	K-Az[1]	K-Az[2]	K-Az[3]	Az^-
				bond distances			
$r(M-N_1)$	2.173	2.636	2.654	2.548	2.945	2.945	
$r(N_1-C_2)$	1.352	1.335	1.335	1.344	1.336	1.336	1.333
$r(C_2-C_3)$	1.397	1.413	1.413	1.400	1.412	1.412	1.409
$r(C_3-C_4)$	1.409	1.413	1.413	1.408	1.412	1.412	1.410
$r(C_4-C_5)$	1.393	1.403	1.403	1.395	1.403	1.403	1.399
$r(C_5-C_6)$	1.406	1.411	1.412	1.406	1.410	1.410	1.408
$r(C_6-C_7)$	1.394	1.405	1.404	1.395	1.403	1.403	1.399
$r(C_7-C_8)$	1.409	1.414	1.414	1.409	1.412	1.412	1.410
$r(C_8-C_9)$	1.398	1.412	1.411	1.400	1.412	1.412	1.409
$r(C_9-N_1)$	1.349	1.335	1.335	1.345	1.336	1.336	1.333
				bond angles			
$\angle MN_1C_2$	100.9	74.0	73.4	101.4	78.5	78.5	
$\angle N_1C_2C_3$	142.0	139.8	139.6	142.0	140.2	140.2	141.1
$\angle C_2C_3C_4$	141.6	141.0	140.9	141.2	141.2	141.2	141.7
$\angle C_3C_4C_5$	139.6	139.5	139.5	139.6	139.6	139.6	139.7
$\angle C_4C_5C_6$	138.5	138.7	138.8	138.7	138.8	138.8	138.5
$\angle C_5C_6C_7$	138.6	138.7	138.7	138.8	138.8	138.8	138.5
$\angle C_6C_7C_8$	139.8	139.7	139.4	139.8	139.6	139.6	139.7
$\angle C_7C_8C_9$	142.1	140.9	140.9	141.6	141.2	141.2	141.7
$\angle C_8C_9N_1$	140.9	139.6	139.6	141.0	140.2	140.2	141.1
$\angle C_9N_1C_2$	136.8	140.9	140.8	137.4	140.0	140.0	138.0
				dihedral angles			
$\angle MN_1C_2C_3$	180.0	47.1	49.4	180.0	49.9	49.8	
$\angle N_1C_2C_3C_4$	0.0	−2.9	−4.3	0.0	2.4	2.3	0.0
$\angle C_2C_3C_4C_5$	0.0	−6.6	−8.1	0.0	−1.8	−2.0	0.0
$\angle C_3C_4C_5C_6$	0.0	2.6	3.0	0.0	−3.4	−3.3	0.0
$\angle C_4C_5C_6C_7$	0.0	6.2	8.0	0.0	−0.1	0.1	0.0
$\angle C_5C_6C_7C_8$	0.0	0.8	1.0	0.0	3.3	3.4	0.0
$\angle C_6C_7C_8C_9$	0.0	−8.9	−8.9	0.0	2.1	1.9	0.0
$\angle C_7C_8C_9N_1$	0.0	−4.5	−5.1	0.0	−2.2	−2.4	0.0
				Mulliken charges			
M	0.82	0.52	0.54	0.91	0.88	0.88	
N_1	−0.38	−0.14	−0.14	−0.40	−0.24	−0.24	−0.27
HOMA	0.953	0.898	0.899	0.953	0.907	0.907	0.92

[a] Bond lengths are in Å and bond angles and dihedral angles are in deg. The Mulliken charges are in au. M = Na or K.

TABLE 8: ^{1}H NMR τ Values (in ppm) of Alkali-Azonide Salts in Different Solvents, Collected from Ref 3

		DMSO	acetone
Li-Az	$\tau_{H_{2(9)}}$	1.50	2.40
	$\tau_{H_{3-8}}$	3.51	3.30
Na-Az	$\tau_{H_{2(9)}}$	1.47	1.74
	$\tau_{H_{3-8}}$	3.45	3.20
K-Az	$\tau_{H_{2(9)}}$	1.36	1.36
	$\tau_{H_{3-8}}$	3.40	3.37

the orbitals of the ring. A similar mechanism is already described for the pyrrolide alkali salts in our paper on pyrrole.[42] The azonide salts differ from the pyrrolide analogues because the σ complexed Na and K salts of azonine are stable minima, whereas the corresponding pyrrolides are transition states. This enhanced stability of the azonides originates probably from the agostic interaction between the metal and the neighboring C−H group. This type of interaction is not possible in pyrrolide because of the sharper polygonal angles in pyrrole that position the hydrogen atoms further away from the metal.

The singlet excitations of K-azonide, solvated in THF, and the calculated singlet excitations of Li-Az[1] are included in Table 4. These values are very similar to the azonine (Et_2O) values, which suggest that the distortion of the azonide frame is similar to that of azonine solvated in Et_2O. The UV−vis spectrum therefore confirms the existence of distorted azonide frames.

The ^{1}H NMR spectra, shown in Table 8, contradict, at first sight, the existence of distorted azonide frames, because the aromaticity is apparently enhanced. Evidence for this enhancement is provided by the large downshift of the τ value of $H_{2(9)}$ and by the coalescence of the remaining hydrogen peaks. The apparent contradiction is easily lifted for the DMSO results. DMSO is a strong cation binding agent and the solvated azonides exist therefore in their anionic form. The anionic form is highly delocalized and planar, see Table 7, and its aromaticity is therefore more pronounced than that in azonine. This is also indicated by the respective HOMA values of 0.929 and 0.900. The large downshift of the $H_{2(9)}$ τ values originates from the deshielding influence of the free electron pair. This effect is strong because of the shape of the large azonine ring, which has the $H_{2(9)}$ atoms residing close to the free electron pair.

The alkali salts have different $\tau_{H_{2(9)}}$ values when they are solvated in acetone, because the cation remains bounded to azonide. These differences are explained by the same mechanism as for DMSO, because Li, Na, and K reside above the azonide plane and create thereby an anion-like azonide ring. This anion-like behavior of the azonide part is also seen in the C−C bond distance alternation, which is smaller for Li-Az[3], the most distorted structure, than for azonine. Inspection of Table 6 shows that most of the Li-azonide HOMA values are larger than the azonine value, and the corresponding structures are therefore more aromatic. This explains why the τ values of H_{3-8} are coalescent and shifted to values similar to the DMSO results. The $\tau_{H_{2(9)}}$ are shifted less in the Li and Na complexes because the $H_{2(9)}$ atoms of these complexes move away from the free electron pair when they lose their planarity. The distortion of the azonide frame is therefore responsible for the smaller downshifts of the $\tau_{H_{2(9)}}$ values of the Li and Na complexes. This correlates with the dihedral angle $\angle H_2C_2N_1C_9$ as a measure of the interaction between the free electron pair and the $H_{2(9)}$ atoms. Li-Az[3] has $\angle H_2C_2N_1C_9$ values of 10.2° and 23.7°, and Li-Az[2] has values of 6.5° and 13.9°. The analogous quantities for Na are 1.0° and 5.3°, and 0.7° and 4.4°. These values clearly demonstrate that the interaction between the free electron pair and $H_{2(9)}$ is almost similar to that of the anion for the Na salt, but is smaller for the Li salt. The $\tau_{H_{2(9)}}$ values of the Li salt are therefore shifted to a lesser extent.

Analysis of both the UV−vis spectra and the ^{1}H NMR spectra of various alkali salts supports the theoretical conclusion of nonplanar azonine salts. The analysis also contradicts the gegenionhypothesis[3] that was already criticized by Kemps-Jones et al.[43] This hypothesis links the size of the counterions, bonded at the σ position, to the $\tau_{H_{2(9)}}$ shifts. The σ position is actually not the preferable binding site and is situated 6.2 and 12.4 kcal/mol above the most preferential binding site for Li and Na, respectively. It is therefore not likely populated at room temperature. The shifts are connected with the size of the counterions, but this is because larger cations also flatten the ring more, which results in lower $\tau_{H_{2(9)}}$ values, and not because of their deshielding influence in the σ position.

4. Conclusions

This is the first detailed theoretical study of azonine, *N*-methylazonine, and the azonide alkali salts. The present study also incorporates the effect of polar solvation media on azonine and *N*-methylazonine. The geometries, potential energy surfaces, singlet excitation energies, and NICS values of azonine and its derivatives have been determined.

Azonine is thus treated as a planar molecule that loses its planarity when it interacts with polar solvents. These results could form an explanation for the ^{1}H NMR study of azonine solvated in acetone that confirmed the existence of both planar

and distorted azonine in the solution.[8] Such a conclusion is supported by the comparison of the UV−vis spectra with the calculated singlet excitation energies. Placing azonine in different solvents has profound effects on the UV−vis spectrum.[4] The theoretical results therefore indicate that the differences between the spectra could be attributed to the existence of distorted azonine complexes.

The UV−vis spectra of *N*-methylazonine and K-azonide show that the azonine frame exists mainly in the distorted form. This planarity loss of *N*-methylazonine and the alkali salts is shown for the first time. The calculated *N*-methylazonine geometries and the corresponding UV−vis spectra and molecular orbitals still support the statement that this heavily distorted molecule is aromatic. The alkali salts, which form π-cation complexes and strongly distort the azonide frame, do remain aromatic. The formation of azonide salts with the metal residing on top of the azonide ring is suggested and proven for the first time. These new results are in accordance with the experimental ^{1}H NMR spectra and contradict the gegenion hypothesis of Anastassiou.[3]

The assignment of the vibrational spectrum of azonines, based on the potential energy distribution concept, is included. The vibrational effects of methylation and binding with water are discussed. The potential energy surface of the rearrangement of azonine to *cis*- and *trans*-8,9-dihydroindole is also derived. It is suggested that the trans form could be formed from azonine when the proper kinetic control is applied.

Acknowledgment. One of the authors, K.R.F.S., gratefully thanks the Flemish Institute for the Promotion of Science-Technology in Industry (IWT) for a grant. E.S.K. and A.C. acknowledge the Scientific Research Council of the University of Leuven for financial support. We also thank Prof. Kris Van Alsenoy of the Universiteit Antwerpen for providing the GAR2PED software.

References and Notes

(1) Anastassiou, A. G.; Gebrian, J. H. *Tetrahedron Lett*. **1970**, *11*, 825.
(2) Anastassiou, A. G.; Eachus, S. W.; Cellura, R. P.; Gebrian, J. H. *Chem. Commun*. **1970**, 1133.
(3) Anastassiou, A. G.; Eachus, S. W. *J. Am. Chem. Soc*. **1972**, *94*, 2537.
(4) Anastassiou, A. G. *Acc. Chem. Res*. **1972**, *5*, 281.
(5) Anastassiou, A. G. *Top. Nonbenzenoid Aromat. Chem.* **1973**, *1*, 1.
(6) Sondheimer, F. *Chimia* **1974**, *28*, 163.
(7) Hückel, E. H. *Grundzüge der Theorie ungesättigter und Aromatischer Verbindungen*; Verlag Chemie: Berlin, Germany, 1938.
(8) Anastassiou, A. G. *Pure Appl. Chem*. **1975**, *44*, 691.
(9) Ouamerali, O.; Gayoso, J. *Int. J. Quantum Chem*. **1986**, *29*, 1599.
(10) Rabinovitz, M.; Cohen, Y. *Tetrahedron* **1988**, **44**, 6957.
(11) Kato, H.; Toda, S.; Arikawa, Y.; Masuzawa, M.; Hashimoto, M.; Ikoma, K.; Wang, S.-Z.; Miyasaka, A. *J. Chem. Soc., Perkin Trans. 1* **1990**, *7*, 2035.
(12) Claramunt, R. M.; Elguero, J.; Katritzky, A. R. *Adv. Heterocycl. Chem*. **2000**, *77*, 1.
(13) Frisch, M. J.; Trucks, G. W.; Schlegel, H. B.; Scuseria, G. E.; Robb, M. A.; Cheeseman, J. R.; Zakrzewski, V. G.; Montgomery, J. A.; Stratmann, R. E.; Burant, J. C.; Dapprich, S.; Millam, J. M.; Daniels, A. D.; Kudin, K. N.; Strain, M. C.; Farkas, O.; Tomasi, J.; Barone, V.; Cossi, M.; Cammi, R.; Mennucci, B.; Pomelli, C.; Adamo, C.; Clifford, S.; Ochterski, J.; Petersson, G. A.; Ayala, P. Y.; Cui, Q.; Morokuma, K.; Malick, D. K.; Rabuck, A. D.; Raghavachari, K.; Foresman, J. B.; Cioslowski, J.; Ortiz, J. V.; Stefanov, B. B.; Liu, G.; Liashenko, A.; Piskorz, P.; Komaromi, I.; Gomperts, R.; Martin, R. L.; Fox, D. J.; Keith, T.; Al-Laham, M. A.; Peng, C. Y.; Nanayakkara, A.; Gonzalez, C.; Challacombe, M.; Gill, P. M. W.; Johnson, B. G.; Chen, W.; Wong, M. W.; Andres, J. L.; Head-Gordon, M.; Replogle, E. S.; Pople, J. A. *Gaussian 98*, Revision A.9; Gaussian, Inc.: Pittsburgh, PA, 1998.
(14) Bettinger, H. F.; Sulzbach, H. M.; Schleyer, P. v. R.; Schaeffer, H. F., III *J. Org. Chem*. **1999**, *64*, 3278.
(15) Califano, S. *Vibrational States*; Wiley: New York, 1985.
(16) Martin, J. M. L. *Mol. Phys*. **1995**, *86*, 1437.
(17) McWeeny, R. *Phys. Rev*. **1962**, *126*, 1028.
(18) Ditchfield, R. *Mol. Phys*. **1974**, *27*, 789.
(19) Wolinski, K.; Hinton, J. F.; Pulay, P. *J. Am. Chem. Soc*. **1990**, *112*, 8251.
(20) Schleyer, P. v. R.; Maerker, C.; Dransfeld, A.; Jiao, H.; van Eikema Hommes, N. J. R. *J. Am. Chem. Soc*. **1996**, 118, 6317.
(21) Krygowski, T. M.; Cyranski, M. K. *Chem. Rev*. **2001**, *101*, 1385,
(22) Roos, B. O. In *Lecture Notes in Chemistry 58, European Summer School in Quantum Chemistry*; Roos, B. O., Ed.; Springer-Verlag: Berlin, Germany, 1992.
(23) Andersson, K.; Malmqvist, P.-Å.; Roos, B. O.; Sadlej, A. J.; Wolinski, K. *J. Phys. Chem*. **1990**, *94*, 5483.
(24) Andersson, K.; Blomberg, M. R. A.; Fülscher, M. P.; Karlström, G.; Lindh, R.; Malmqvist, P.-Å; Neogrády, P.; Olsen, J.; Roos, B. O.; Sadlej, A. J.; Schütz, M.; Seijo, L.; Serrano-Andrés, L.; Siegbahn, P. E. M.; Widmark, P.-O. *Molcas*, Version 4; Lund University: Lund, Sweden, 1997.
(25) Serrano-Andrés, L.; Roos, B. O. *J. Am. Chem. Soc*. **1996**, *118*, 185.
(26) Roos, B. O.; Andersson, K.; Fülscher, M. P.; Malmqvist, P.-Å.; Sérrano-Andres, L.; Pierloot, K.; Merchán, M. *Adv. Chem. Phys*. **1996**, *93*, 219.
(27) Salcedo, R.; Martinez, A.; Sansores, L. E. *Tetrahedron* **2001**, *57*, 8759.
(28) Harrison, R. D. *Book of Data*; Longman Group UK Limited: Essex, UK, 1995.
(29) Steiner, E.; Fowler, P. W.; Havenith, R. W. A. *J. Chem. Phys*. **2002**, *106*, 7048.
(30) Somers, K. R. F.; Kryachko, E. S.; Ceulemans, A. *Chem. Phys*. In press.
(31) Andersson, K.; Barysz, M.; Bernhardsson, A.; Blomberg, M. R. A.; Cooper, D. L.; Fülscher, M. P.; de Graaf, C.; Hess, B. A.; Karlström, G.; Lindh, R.; Malmqvist, P.-Å; Nakajima, T.; Neogrády, P.; Olsen, J.; Roos, B. O.; Schimmelpfennig, B.; Schütz, M.; Seijo, L.; Serrano-Andrés, L.; Siegbahn, P. E. M.; Stålring, J.; Thorsteinsson, T.; Veryazov, V.; Widmark, P.-O. *Molcas*, Version 5.4; Lund University: Lund, Sweden, 2002.
(32) Chiang, C. C.; Paul, I. C.; Anastassiou, A. G.; Eachus, S. W. *J. Am. Chem. Soc*. **1974**, *96*, 1636.
(33) Crabtree, R. H. *Angew. Chem., Int. Ed. Engl*. **1993**, *32*, 789.
(34) Popelier, P. L. A.; Logothetis, G. *J. Organomet. Chem*. **1998**, *555*, 101.
(35) Desiraju, G. R.; Steiner, T. *The Weak Hydrogen Bond*; Oxford University Press: London, UK, 1999.
(36) Caldwell, J. W.; Kollman, P. A. *J. Am. Chem. Soc*. **1995**, *117*, 4177.
(37) Mecozzi, S.; West, A. P.; Dougherty, D. A. *Proc. Natl. Acad. Sci. U.S.A.* **1996**, *93*, 10566.
(38) Mecozzi, S.; West, A. P.; Dougherty, D. A. *J. Am. Chem. Soc*. **1996**, *118*, 2307.
(39) Ma, J. C.; Dougherty, D. A. *Chem. Rev*. **1997**, *97*, 1303.
(40) Feller, D. *Chem. Phys. Lett*. **2000**, *322*, 543.
(41) Tsuzuki, S.; Yoshida, M.; Uchimaru, T.; Mikami, M. *J. Phys. Chem. A* **2001**, *105*, 769.
(42) Somers, K. R. F.; Kryachko, E. S.; Ceulemans, A. *J. Phys. Chem. A* **2003**, *107*, 5427.
(43) Kemps-Jones, A. V.; Jones, A. J.; Sakai, M.; Beeman, C. P.; Masamune, S. *Can. J. Chem*. **1973**, *51*, 767.